The EMBO Journal vol.7 no.11 pp.3577 - 3587, 1988

The importance of highly conserved nucleotides in the binding region of chloramphenicol at the peptidyl transfer centre of *Escherichia coli* 23S ribosomal RNA

Birte Vester and Roger A.Garrett

Biostructural Chemistry, Kemisk Institut, Aarhus Universitet, DK-8000 Aarhus C, Denmark

Communicated by R.A.Garrett

The peptidyl transfer site has been localized at the centre of domain V of 23S-like ribosomal RNA (rRNA) primarily on the basis of a chloramphenicol binding site. The implicated region constitutes an unstructured circle in the current secondary structural model which contains several universally conserved nucleotides. With a view to investigate the function of this RNA region further, four of these conserved nucleotides, including one indirectly implicated in chloramphenicol binding, were selected for mutation in *Escherichia coli* 23S rRNA using oligonucleotide primers. Mutant RNAs were expressed *in vivo* on a plasmid-encoded rRNA (*rrn*B) operon and each one yielded dramatically altered phenotypes. Cells exhibiting $A_{2060} \rightarrow C$ or $A_{2450} \rightarrow C$ transversions were inviable and it was shown by inserting the mutated genes after a temperature-inducible promoter that the mutant RNAs were directly responsible. In addition, a $G_{2502} \rightarrow A$ transition caused a decreased growth rate, probably due to a partial selection against mutant ribosome incorporation into polysomes, while an $A_{2503} \rightarrow C$ transversion produced a decreased growth rate and conferred resistance to chloramphenicol. All of the mutant RNAs were incorporated into 50S subunits, but while the two lethal mutant RNAs were strongly selected against in 70S ribosomes, the plasmid-encoded $A_{2503} \rightarrow C$ RNA was preferred over the chromosome-encoded RNA, contrary to current regulatory theories. The results establish the critical structural and functional importance of highly conserved nucleotides in the chloramphenicol binding region. A mechanistic model is also presented to explain the disruptive effect of chloramphenicol (and other antibiotics) on peptide bond formation at the ribosomal subunit interface.

Key words: conserved nucleotides/23S ribosomal RNA/primer-directed mutagenesis/chloramphenicol/peptidyl transfer

Introduction

The direct involvement of rRNA sites in ribosomal function was first inferred by Noller and Chaires (1972) who demonstrated that 16S RNA participated directly in tRNA binding. This finding was reinforced by evidence for mRNA binding directly to 16S RNA (Shine and Dalgarno, 1974; Jacob *et al.*, 1987) and has received support from the finding that cytotoxins act at RNA sites (Senior and Holland, 1971; Endo and Wool, 1982; Endo *et al.*, 1987) and from detailed characterization of tRNA and antibiotic binding sites (Moazed and Noller, 1986, 1987a,b and references therein). Many of the functionally important RNA regions have been localized within the most recent secondary structural model, and they frequently correspond to conserved sequence regions that are accessible on the ribosome and are susceptible to post-transcriptional modification (reviewed by Noller, 1984). Unfortunately, a more detailed understanding of the functional roles of the RNA is severely limited by a lack of knowledge of its higher-order structure.

The peptidyl transfer site is probably the most important functional site in the ribosome and it has been localized at the centre of domain V in *Escherichia coli* 23S RNA in a region containing several universally conserved nucleotides (reviewed by Noller, 1984). The site is defined by a group of single nucleotide mutations which are associated with the binding of chloramphenicol and anisomycin, both of which inhibit peptidyl transfer (reviewed by Vazquez, 1979). Erythromycin and related MLS-type antibiotics, which interfere with chloramphenicol binding to ribosomes, but do not block peptidyl transfer directly (Pestka, 1974), also bind in this region. Furthermore, a site within this region formed a cross-link with the 3′ end of an analogue of Phe-tRNA (Barta *et al.*, 1984).

In the present study, four nucleotides that are indicated in the centre of Figure 1 were selected for mutation. They are all universally conserved (i.e. they are conserved in all known sequences). One (A_{2503}) corresponds to a site that has been implicated indirectly in the chloramphenicol-resistance phenotype of yeast mitochondria while the other three (A_{2060}, A_{2450} and G_{2502}) all lie adjacent to nucleotides associated with the chloramphenicol-resistance phenotype in different eukaryotic mitochondria (Figure 1). The nucleotides were altered with a view to investigate the functional importance of universal nucleotides located at the peptidyl transferase centre of the ribosome.

Results

Construction of mutant plasmids

pDV was derived from the multicopy plasmid pKK3535 (Brosius *et al.*, 1981) by deleting two fragments to simplify subsequent cloning steps. It contained the complete *rrn*B rRNA operon of *E.coli* and was used both as a control plasmid and as a cloning vehicle.

Prior to mutagenesis most of the rRNA operon was deleted to yield the small plasmid pSV (Figure 2A) which contained only domains V and VI of 23S RNA. Thus any deleterious effects resulting from expression of mutated 23S RNA could be avoided. After annealing, primer extension and ligation, the plasmid was transformed into competent HB101 cells of *E.coli*. Transitions and transversions were introduced using the experimental procedure outlined in Figure 2. Colonies were transferred to filters and screened for each mutation; mutant yields were ~10%. The 'gapped-duplex'

©IRL Press Limited, Oxford, England

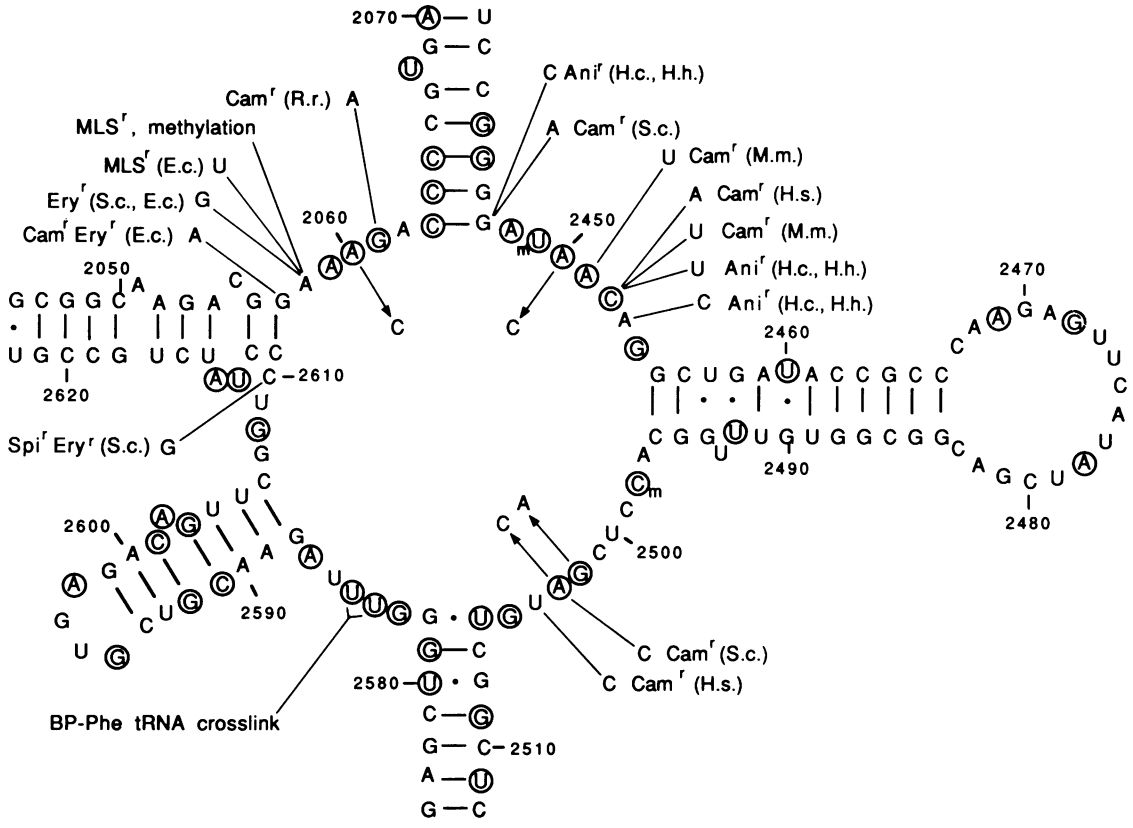

Fig. 1. Secondary structure of the central part of domain V in *E.coli* 23S RNA as derived from phylogenetic sequence comparisons (reviewed by Noller, 1984). Encircled nucleotides are completely conserved in the 23S-like RNAs of 28 organisms from eukaryotes, archaebacteria and eubacteria (Leffers *et al.*, 1987; N.Larsen and H.Leffers, unpublished results). Literature data on natural mutations or *in vitro* induced mutations, and chemically reactive or cross-linked sites are indicated outside the circle. Data from the present study are shown inside the circle. All of the eukaryotic mutants were characterized for mitochondrial rRNAs. The following mutations are indicated: $G_{2057} \rightarrow A$ (*E.coli*: Ettayebi *et al.*, 1985), $A_{2058} \rightarrow m_2A$ (*Streptomyces erythraeus*: Skinner and Cundliffe, 1982), $A_{2058} \rightarrow U$ (*E.coli*: Sigmund *et al.*, 1984), $A_{2058} \rightarrow G$ (*E.coli*: Vester and Garrett, 1987; *Saccharomyces cerevisiae*: Sor and Fukuhara, 1982), $G_{2061} \rightarrow A$ (*Rattus rattus*: Koike *et al.*, 1983), $G_{2447} \rightarrow C$ (*Halobacterium halobium, Halobacterium cutirubrum*: Hummel and Böck, 1987), $G_{2447} \rightarrow A$ (*S.cerevisiae*: Dujon, 1980), $A_{2451} \rightarrow U$ (*Mus mus*: Kearsey and Craig, 1981), $C_{2452} \rightarrow A$ (*Homo sapiens*: Blanc *et al.*, 1981), $C_{2452} \rightarrow U$ (*H.halobium, H.cutirubrum*: Hummel and Böck, 1987; *M.mus*: Slott *et al.*, 1983), $A_{2453} \rightarrow C$ (*H.halobium, H.cutirubrum*: Hummel and Böck, 1987), $A_{2503} \rightarrow C$ (*S.cerevisiae*: Dujon, 1980), $U_{2504} \rightarrow C$ (*H.sapiens*: Kearsey and Craig, 1981; Blanc *et al.*, 1981) and $C_{2611} \rightarrow G$ (*S.cerevisiae*: Sor and Fukuhara, 1984). The numbers refer to corresponding nucleotide positions in the *E.coli* 23S RNA. An affinity labelled site for benzophenone(BP)-derivatized Phe-tRNA is also shown (Barta *et al.*, 1984).

method was used to simplify the back-cloning procedure which was otherwise complicated by a paucity of unique, and useable, restriction sites in the 23S RNA gene. The mutated DNA was then digested with *Pvu*II and *Pst*I and recloned into pDV.

The integrity of the mutations was verified by cloning the appropriate DNA fragment from the small non-expressed plasmids, and expression plasmids, into M13mp18/19 vectors for DNA sequencing, or the region was sequenced directly on the plasmid. The results are presented in Figure 3.

All four mutations dramatically reduced the cell growth rate

Plasmids containing each of the four mutations in the *rrn*B operon were transformed into strain HB101 cells. Cells carrying the $A_{2060} \rightarrow C$ and $A_{2450} \rightarrow C$ mutations failed to produce colonies and it was inferred that both mutations were lethal (and this is confirmed below). In contrast, HB101 cells bearing the mutations $G_{2502} \rightarrow A$ (pDV4) and $A_{2503} \rightarrow C$ (pDV3) yielded small colonies on agar plates and exhibited much slower doubling times (59 and 79 min respectively) than cells containing control plasmid pDV (40 min). The reduced growth rate of all the mutants suggested that less active or inactive mutated ribosomes slowed down or blocked protein biosynthesis. Moreover, this decreased growth rate was accentuated for colonies stored on agar plates (at 4°C), presumably because defective ribosomes accumulated and inhibited the restart of growth.

Expression of the $A_{2060} \rightarrow C$ and $A_{2450} \rightarrow C$ mutant RNAs was lethal

The effect of expression of the two mutated RNAs on cell viability was investigated further by cloning the DNA fragment from pSV (Figure 2) into pLK35, a derivative of pNO2680 (Gourse *et al.*, 1985) containing a λP_L promoter/operator before the *rrn*B operon. The cloning produced a small deletion downstream from the T_1 and T_2 terminators (see Materials and methods). The new construct pLK35V contained the unmutated fragment and was similar to pDV except for the exchanged promoter and the addition of the DNA fragment from pBR322 in the reverse orientation relative to the rRNA operon. pLK35V5 and pLK35V2 carrying the $A_{2060} \rightarrow C$ and $A_{2450} \rightarrow C$ mutations, respectively, were constructed in a similar manner. All plasmids were sequenced through the mutated position to ensure that no recombination had occurred (Figure 3).

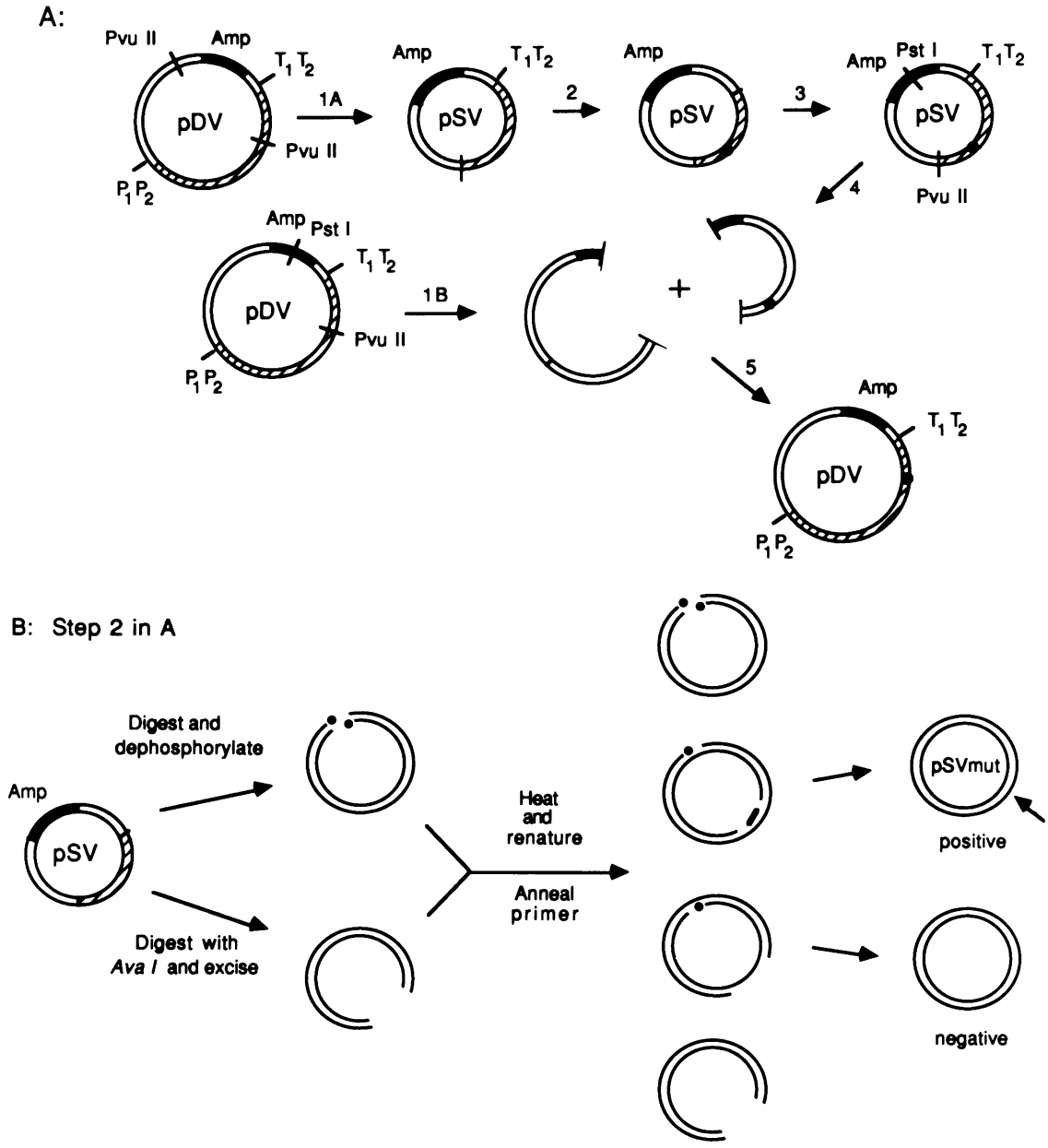

Fig. 2. (**A**) An outline of the strategy for constructing a mutant plasmid pDV_{mut} from pDV. The restriction enzyme sites used for fragmentation are indicated and the mutated position is denoted by a black dot. P_1, P_2 and T_1, T_2 refer to promoters and terminators, respectively, from the *rrn*B operon. (**B**) The procedure for introducing the mutation (step 2 in A) is shown in detail. Dots represent dephosphorylated ends. The mutagenic-primer was hybridized to the ssDNA gap and extended by the Klenow enzyme in the presence of dNTPs. The ends were then ligated to yield circular DNA prior to transformation. Colonies were screened for mutants by dot-blotting. Experimental details are given in Materials and methods.

The effects of the mutation *in vivo* were then investigated using a conditional rRNA expression system. Host cells carried a heat-sensitive λ repressor (C_{600} and M5219) which would repress the plasmid-encoded rRNA genes at 30°C but was inactivated at 42°C. The plasmid constructs were first transformed into strain C_{600} in order to accrue a high yield of plasmids. These were then isolated and retransformed into strain M5219 for further study (Gourse *et al.*, 1985).

The effects of the mutations on growth curves were measured at 30°C and then at 42°C for the control plasmid pLK35V and the mutated plasmids pLK35V5 (A_{2060} → C) and pLK35V2 (A_{2450} → C). Expression of the mutant rRNAs at 42°C produced a large decrease in the cell growth rate (Figure 4). A similar result was also obtained by spreading diluted cell cultures grown at 30°C on agar plates and incubating half at 30°C and half at 42°C. At 30°C, colonies containing mutated plasmids appeared similar to those with control plasmids. At 42°C, however, no colonies appeared for cells containing mutant rRNA while colonies of cells producing plasmid-expressed control rRNA were small (data not shown).

Control experiments were performed to establish whether the failure to produce colonies of HB101 cells after transforming with mutated plasmids was, indeed, due to expression of mutated 23S RNA. The control plasmid pLK35V and the mutated plasmids pLK35V5 (A_{2060} → C) and pLK35V2 (A_{2450} → C) were each transformed, simultaneously, into strains HB101 and C_{600}. The numbers

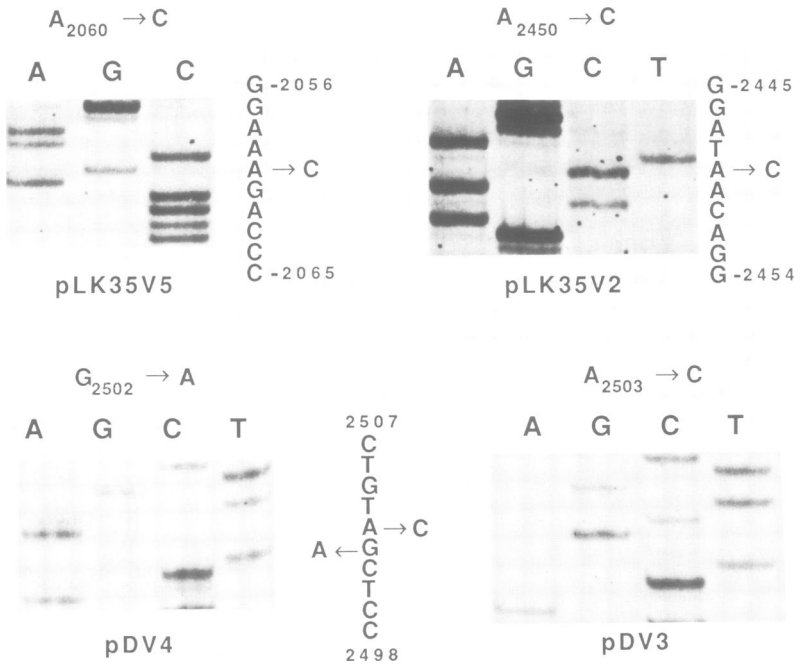

Fig. 3. DNA sequence evidence for the accuracy of the mutations in plasmids pLK35V5 (A_{2050} → C), pLK35V (A_{2450} → C), pDV4 (G_{2502} → A) and pDV3 (A_{2503} → C). Mutated positions are indicated. The nucleotide positions in the 23S RNA of *E.coli* (Figure 1) are given.

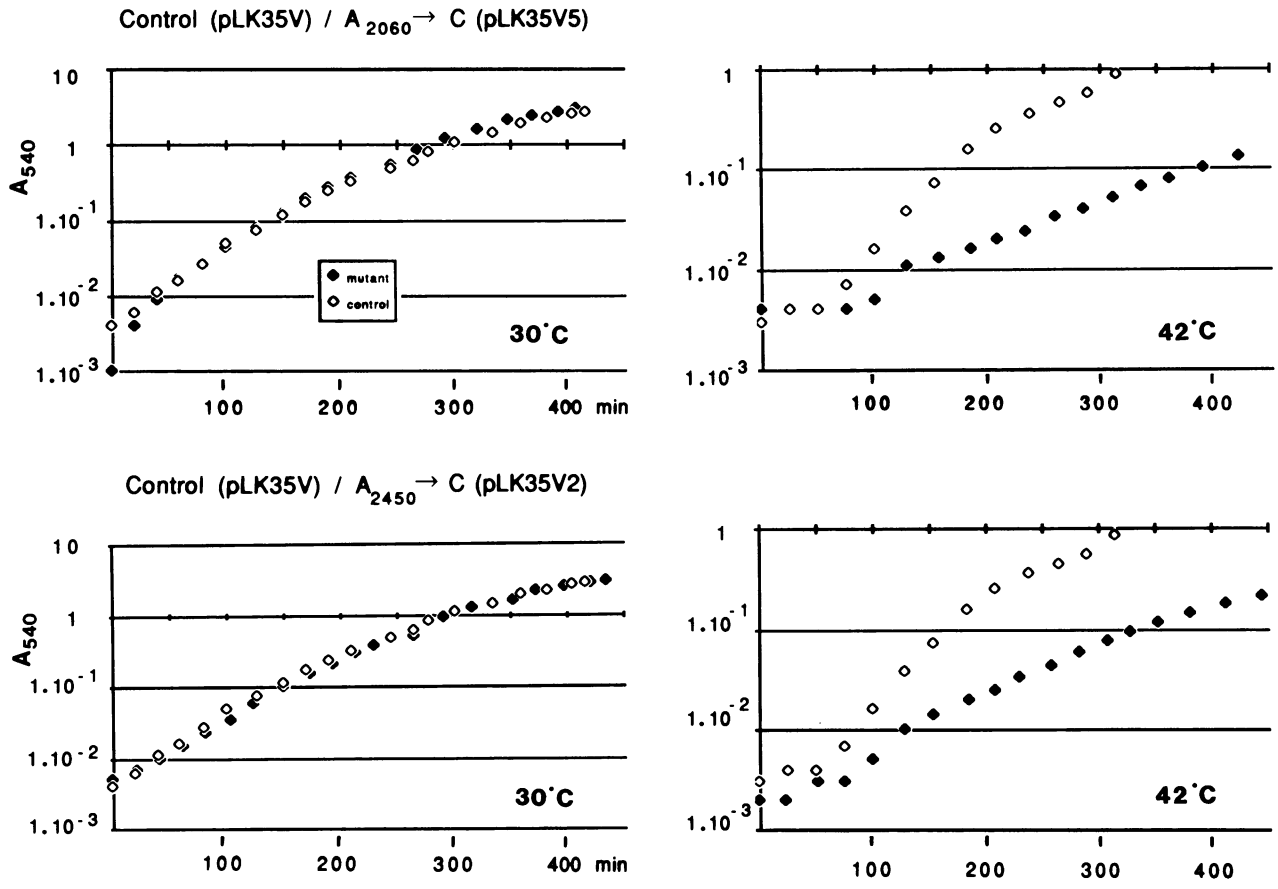

Fig. 4. Growth curves for M5219 cells containing the control plasmid pLK35V (○) and the mutated plasmids pLK35V2 and pLK35V5 (●) grown in LB media containing 50 μg/ml ampicillin and measured at 30°C and 42°C.

of colonies that formed were determined and compared, and are listed in Table I. The plasmid-encoded RNAs were expressed normally in HB101 cells, while in C_{600} cells, which were maintained at 30°C, these genes were repressed. Thus, if there was no deleterious effect of the expressed mutant RNA, the colony ratio HB101:C_{600} would be the same for the control and the two mutant plasmids. However, both the long lag phase and the small number of viable colonies (Table I) confirmed that the mutated RNA had a major deleterious effect on growth of strain HB101 (Table I).

Chloramphenicol phenotypes for the G_{2502} → A and A_{2503} → C mutants

An A_{2503} → C mutation is associated with chloramphenicol resistance in yeast mitochondria (Figure 1), and we therefore investigated whether the same, or the adjacent G_{2502} → A mutation produced a chloramphenicol-resistance phenotype in *E.coli*. HB101 cells that were transformed with pDV3 (A_{2503} → C) grew at much higher antibiotic concentrations than control cells containing pDV (Table II). Thus, the mutated, plasmid-derived, 23S RNA was incorporated into functional ribosomes to yield a chloramphenicol-resistant phenotype. In contrast, HB101 cells carrying the G_{2502} → A mutation on plasmid pDV4 exhibited no chloramphenicol resistance relative to cells containing pDV.

How much mutant RNA is incorporated into ribosomes in vivo

The effect of each mutation on ribosomal assembly and function was investigated by isolating ribosomes and separating ribosomes and subunits on sucrose gradients as shown in Figure 5 for the A_{2503} → C mutant. The ratio of mutant:wild-type RNA present in the peaks was then estimated approximately from RNA sequencing gels obtained using primer-directed reverse transcription (Figure 6). The results are summarized in Table III.

Table I. Control transformation of 'lethal' plasmids into HB101/cells

	E.coli strain		
	C_{600}	HB101	C_{600}:HB101
Incubation time (h)	20	20 46	
pLK35V (control)	97	87 87	1.1:1
pLK35V5 (A_{2050} → C)	445	0 12	37:1
pLK35V2 (A_{2450} → C)	272	0 11	25:1

The number of colonies are given that were visible on agar plates after transformation.

Table II. Effect of chloramphenicol on the doubling time (min) of *E.coli* HB101 cells containing plasmids pDV (control) and pDV3 (A_{2503} → C)

Plasmid	Chloramphenicol (μg/ml)					
	0	4	7	10	15	20
pDV (control)	40	–	–	–	–	–
pDV3 (A_{2503} → C)	79	96	110	120	151	198

Cultures containing 50 μg/ml ampicillin and increasing amounts of chloramphenicol were grown overnight at 37°C. They were diluted to ~0.2 A_{240} units and the growth rate was determined over at least three doubling times.

M5219 cells containing mutated plasmids pLK35V5 (A_{2060} → C) and pLK35V2 (A_{2450} → C) were grown to mid-log phase at 30°C and then the temperature was raised and maintained at 42°C for 2 h to induce expression of the mutated rRNA. Cells were harvested and the ribosomes were isolated and examined on sucrose gradients. RNA sequencing by reverse transcriptase demonstrated that the A_{2060} → C mutated RNA was incorporated into 70S ribosomes at a low level (Table III) which suggested that the mutation impaired 50S subunit assembly and function. No A_{2450} → C mutated RNA was detected in the 70S ribosome peak but it was present in the 50S subunit peak (Table III). This implied that the mutation impaired 50S subunit assembly and/or 30S-50S subunit association.

The G_{2502} → A mutant ribosomes were isolated on Sephacryl S-200 columns and the major part of the peak was pooled and analysed on sucrose gradients. Densitometry of

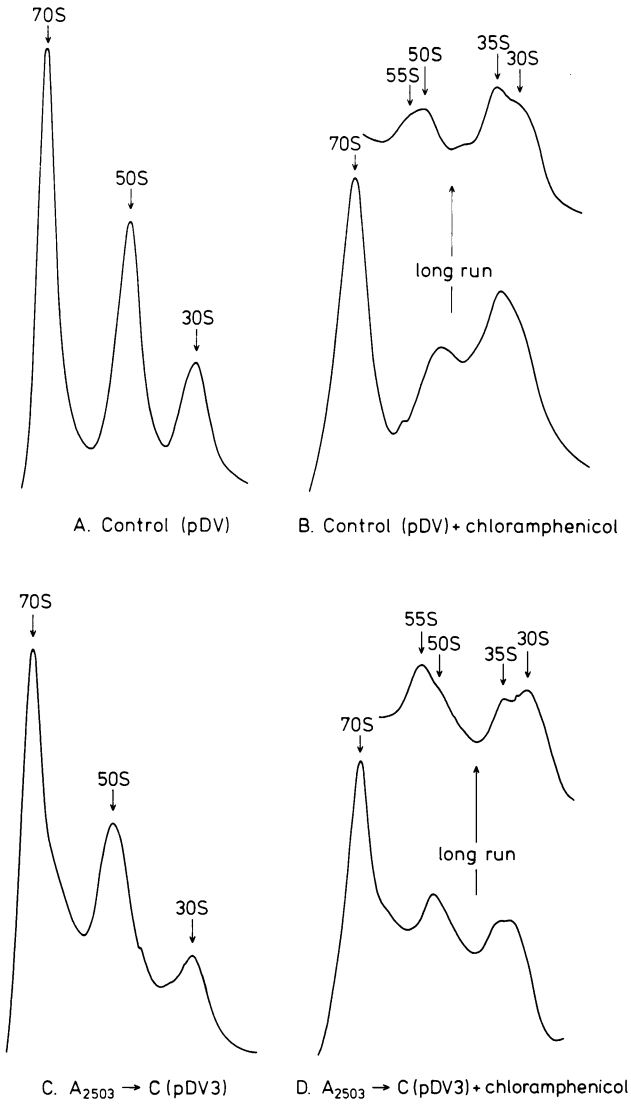

Fig. 5. Elution profiles from sucrose gradients of ribosome preparations. Cells containing control pDV were grown in the absence (**A**) and presence (**B**) of 4 μg/ml chloramphenicol. Cells containing pDV3 (A_{2503} → C) were grown in the absence (**C**) and presence (**D**) of 7.5 μg/ml chloramphenicol. The position of the ribosomal and subunit peaks are indicated by arrows.

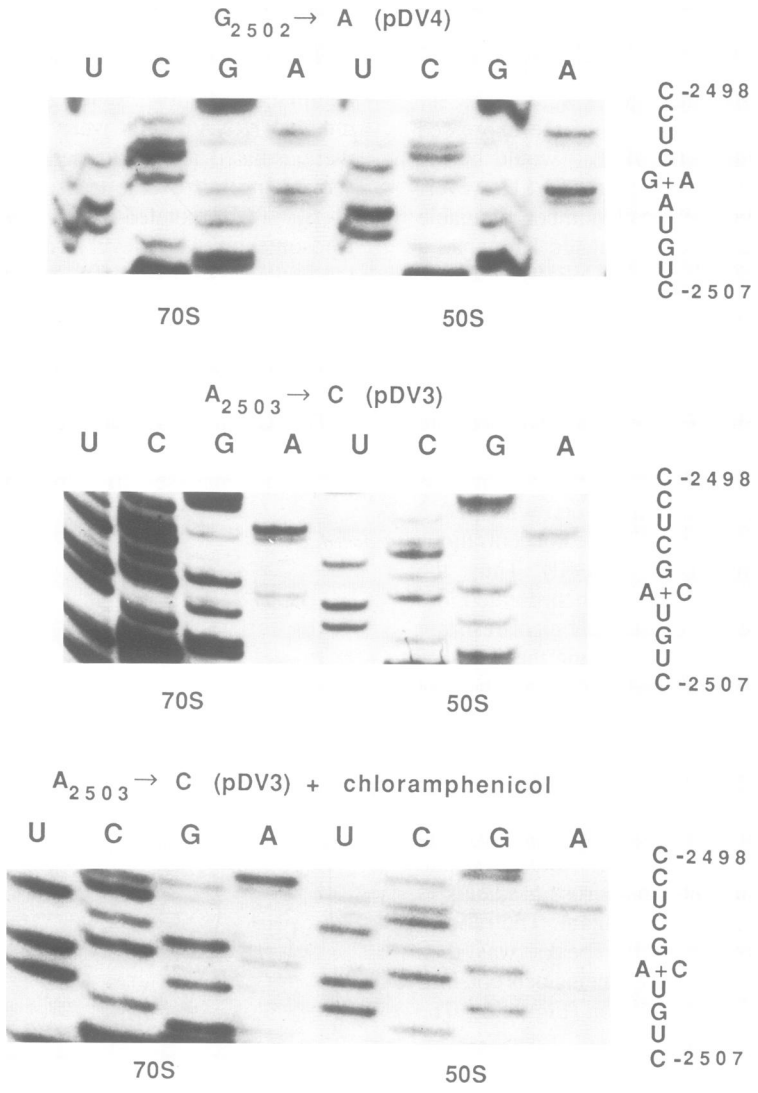

Fig. 6 RNA sequence evidence for the incorporation of mutated RNA into ribosomes. RNA was derived from cells containing pDV4 (G_{2502} → A) and pDV3 (A_{2503} → C) grown in the absence and presence of chloramphenicol. RNA was isolated from 70S ribosomes and 50S subunits that were separated on sucrose gradients and sequenced through the mutated position with reverse transcriptase. The nucleotide tracks are denoted by U, C, G and A. Arrows indicate the bands produced by a mixture of wild-type and mutated 23S RNA.

autoradiograms of sequencing gels revealed ~50% mutant RNA in both 50S subunits and 70S ribosomes (Figure 6; Table III). In contrast, for the A_{2503} → C mutant, a very high level of mutant RNA (>90%) was present in both 50S subunits and 70S ribosomes from cells grown in the absence and presence of chloramphenicol (Figure 6; Table III).

For the A_{2503} → C mutant, we also investigated whether chloramphenicol affected the assembly or stability of 70S ribosomes. Cells containing control plasmid pDV were grown to mid-log phase and then incubated for 1 h with 4 μg/ml chloramphenicol while cells containing pDV3 (A_{2503} → C) were grown in 7.5 μg/ml chloramphenicol. Complex ribosomal profiles are shown for both cell types in Figure 5. The important result is that all chloramphenicol-treated ribosomes exhibited additional peaks migrating at ~55S and ~35S (Figure 5B,D). Since these sedimentation values correspond to particles that are larger or more

Table III. Incorporation of mutant RNAs into ribosomes *in vivo*

Mutant	% incorporation in 50S subunits	% incorporation in 70S ribosomes
A_{2060} → C	50 (± 10)	10 (± 5)
A_{2450} → C	60 (± 10)	<10
G_{2502} → A	50 (± 10)	55 (± 10)
A_{2503} → C	>90	>90

The percentage of mutant RNA was estimated by densitometry of reverse transcriptase tracks on autoradiograms. RNA mixtures containing chromosome-encoded wild-type and plasmid-encoded mutant RNA was extracted from 50S subunits and 70S ribosomes respectively. Peaks corresponding to the mutated nucleotide bands were normalized relative to neighbouring peaks, and the relative decrease in the wild-type nucleotide band and increase in the mutant nucleotide was estimated. The error limits reflect variations in the results from experiment to experiment <10% and >90% indicate that only one nucleotide (wild-type or mutant) was detected.

Table IV. Reactivity of nucleotides within the centre of domain V in control and mutant 23S RNAs from 70S ribosomes

Nucleotides	Ribonucleases or chemical reagents	Control	Modification	
			$G_{2502} \rightarrow A$	$A_{2503} \rightarrow C$
A_{2051}	RNase CV	(+)	(+)	(+)
C_{2055}	RNase CV	(+)	(+)	(+)
C_{2055}	DMS	(+)	(+)	(+)
A_{2058}	DMS	++	++	++
A_{2059}	DEP	+	+	+
A_{2059}	DMS	++	++	++
A_{2060}	DEP	+	+	+
A_{2060}	DMS	(+)	(+)	(+)
G_{2061}*	Kethoxal	+	(+)	+
G_{2502}	DMS	−	+	−
A_{2503}	DEP	+	+	−
U_{2506}	CMCT	++	++	++
G_{2505}	Kethoxal	−	−	+
G_{2505}	CMCT	+	+	+
A_{2062}	DEP	+	+	+
A_{2062}	DMS	++	++	++
C_{2064}	RNase CV	(+)	(+)	(+)
C_{2065}	RNase CV	+	+	+
U_{2068}	CMCT	+	+	+
A_{2450}	DEP	(+)	(+)	(+)
A_{2453}*	DEP	(+)	+	+
G_{2454}	Kethoxal	+	+	+
C_{2466}	RNase CV	+	+	+
A_{2468}	DMS	++	++	++
A_{2469}	DMS	++	++	++
U_{2473}	CMCT	++	++	++
U_{2474}	CMCT	++	++	++
A_{2476}	RNase T_2	+	+	+
A_{2476}	DEP	++	++	++
A_{2476}	DMS	++	++	++
U_{2477}	CMCT	(+)	(+)	(+)
A_{2478}	DMS	+	+	+
A_{2482}	DMS	++	++	++
C_{2483}	DMS	+	+	+
U_{2491}	CMCT	+	+	+
U_{2493}	CMCT	+	+	+
G_{2502}*	DMS	−	+	−
A_{2503}*	DEP	+	+	−
G_{2505}*	Kethoxal	−	−	+
U_{2506}	CMCT	++	++	++
G_{2576}	RNase CV	+	+	+
U_{2584}	CMCT	+	+	+
U_{2585}	CMCT	++	++	++
U_{2586}	CMCT	+	+	+
A_{2587}	RNase T_2	(+)	(+)	(+)
A_{2587}	DEP	+	+	+
A_{2587}	DMS	(+)	(+)	(+)
A_{2590}	RNase CV	++	++	++
U_{2596}	CMCT	(+)	(+)	(+)
G_{2597}	Kethoxal	(+)	(+)	(+)
A_{2600}	RNase CV	+	+	+
A_{2602}	DEP	+	+	+
A_{2602}	DMS	(+)	(+)	(+)
G_{2603}	Kethoxal	(+)	(+)	(+)

The $G_{2502} \rightarrow A$ and $A_{2503} \rightarrow C$ mutant ribosomes contained ~50% and >90% mutant RNA respectively. The reactive sites were identified by the reverse transcriptase procedure. Nucleotides that exhibited altered reactivities in the mutant ribosomes are indicated by asterisks. Modifications and ribonuclease cuts were quantified visually and were graded according to the following scale: ++ strong, + medium, (+) weak, − no reactivity.

compact than normal subunits, we inferred that they must result from ribosomes dissociating during centrifugation. In a control experiment, the possibility that the extra peaks resulted from ribosome-bound chloramphenicol was eliminated by growing cells without chloramphenicol and then running the ribosomes in sucrose gradients containing chloramphenicol.

The disproportionately large 30S peak could reflect the presence of co-sedimenting 'chloramphenicol particles' which overlap with the tail region of this peak. These particles constitute precursor 16S and 23S RNAs that are probably complexed with a mixture of ribosomal protein and soluble cellular protein (Schleif, 1968). This possibility was investigated by analysing the 16S precursor RNA content of each sucrose gradient fraction on 2.5% polyacrylamide gels. The precursor RNA was, indeed, shown to be concentrated exclusively in the tail region of the 30S peak and constituted ~30% of the total RNA in that part of the peak. Analysis of the protein compositions of the same gradient fractions revealed only ribosomal proteins throughout all peak fractions (data not shown).

In summary, the results for each mutant were different. All were incorporated into 50S subunits, but subunits containing the $A_{2060} \rightarrow C$ and $A_{2450} \rightarrow C$ RNAs were strongly selected against in 70S ribosome formation, while the other mutants were incorporated at normal ($G_{2502} \rightarrow A$), and very high levels ($A_{2503} \rightarrow C$), into both 50S subunits and 70S ribosomes.

RNA structure at the centre of domain V

For the $G_{2502} \rightarrow A$ and $A_{2503} \rightarrow C$ mutants the cells were viable and sufficiently high levels of mutated RNA were present in the ribosomes (50% and >90% respectively) to permit a structural analysis of the mutated RNA region. Therefore, with a view to gain insight into the structural alterations induced in the RNA region by the mutations, the region was probed in the wild-type and mutated ribosomes. The following ribonucleases and chemical reagents were used and the detailed procedures described by Egebjerg *et al.* (1987) were followed: RNase T_2 (single-strand specific), RNase CV (double-strand specific), DEP (adenosine, N-7), DMS (adenosine, N-1 and cytidine, N-3), Kethoxal (guanosine, N-1 and N-2) and CMCT (uridine, N-3 and guanosine, N-1). Reactive sites were analysed by a reverse transcriptase procedure (Moazed *et al.*, 1986) and identified by co-electrophoresing RNA sequencing samples.

The results are averaged and summarized in Table IV and superimposed on the secondary structure model in Figure 7. Only minor changes in reactivity were observed for each mutant that included the mutated nucleotides. Enhanced DEP reactivity at A_{2453} was common to both mutant RNAs and, in addition, Kethoxal reactivity was reduced at G_{2061} for the $G_{2502} \rightarrow A$ mutant and increased for the $A_{2503} \rightarrow C$ mutant at G_{2505}.

Functional activity of the mutant ribosomes

The preceding results demonstrated that mutations $A_{2060} \rightarrow C$ and $A_{2450} \rightarrow C$ produced ribosomes that can be considered inactive, while the $A_{2503} \rightarrow C$ mutation yielded ribosomes that were definitely active in the presence of chloramphenicol. Since no ribosome function data were available for the $G_{2502} \rightarrow A$ mutant, polysomes from this

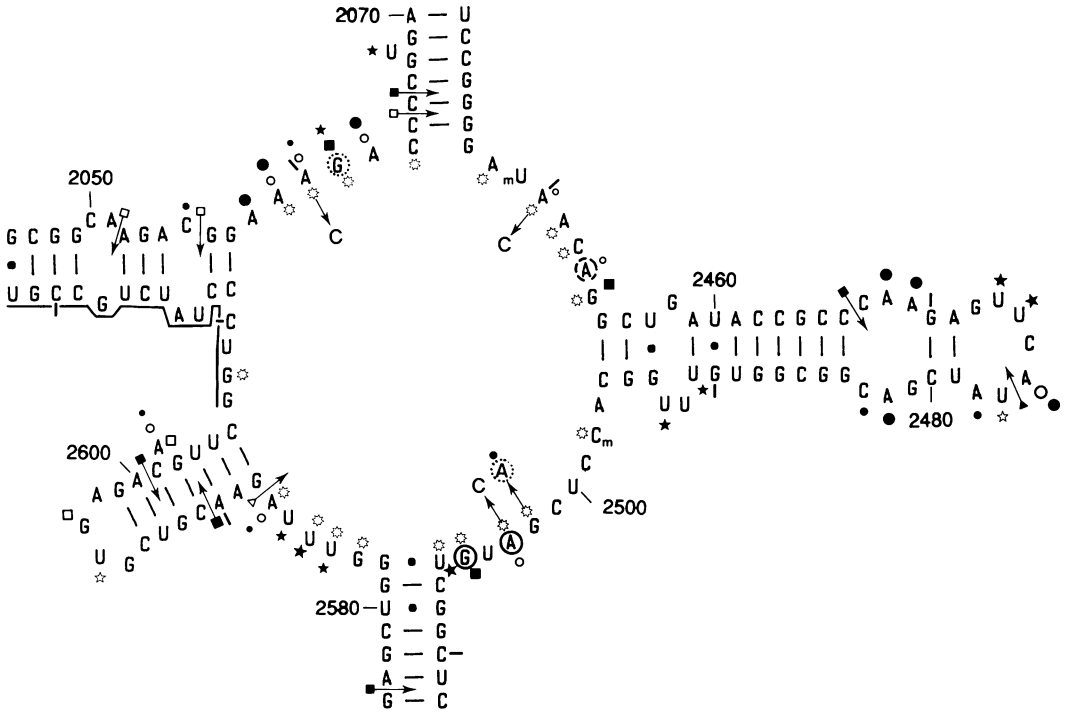

Fig. 7. Accessible nucleotides in the centre of domain V. Chemical modification and ribonuclease cutting data are from Table IV. Increasing degrees of reactivity, (+), +, ++, respectively are represented as follows: RNase T_2 ▷→▶ ; RNase CV □→■→■ ; DEP ○○○ ; DMS ●●● ; CMCT ☆★★ ; Kethoxal □ ■. Conserved nucleotides in the central circle, only, are denoted by an asterisk inside the circle. The mutations are shown by arrows. Nucleotides with different reactivities between control and mutant samples are denoted by ⁘ for G_{2502} → A and by ○ for A_{2503} → C. A_{2453} was altered in both.

mutant were isolated on sucrose gradients and analysed for their 23S RNA composition using the sequencing and densitometry procedures described above. Polysomes exhibiting four or more ribosomes per mRNA were pooled. Analyses from two independent experiments revealed that they contained ~40% mutated RNA and we inferred, therefore, that the mutant ribosomes were active. Moreover, this analysis provided some insight into the reason for the decreased cellular growth rate of this mutant since the percentage of mutant RNA was significantly lower in the polysomes (40%) than in the free ribosomes (55%; Table III), suggesting some selection against uptake of the mutant ribosomes into polysomes.

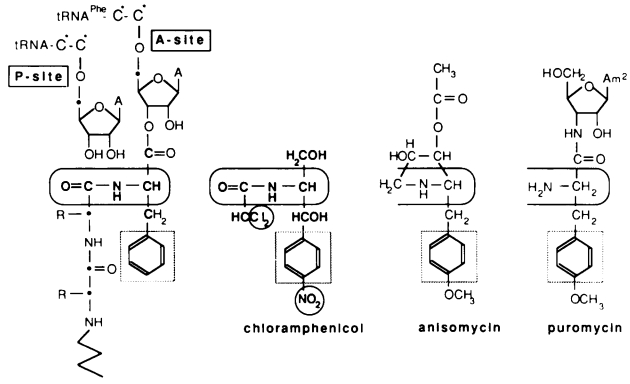

Fig. 8. Hypothetical model for the mechanism of chloramphenicol inhibition of peptide bond formation at the peptidyl transfer centre. The iso-structural regions of chloramphenicol, anisomycin and puromycin are boxed. In order to simplify the tRNA-peptide structure some carbon atoms are represented by dots and their bound H atoms are omitted. The C* represents cytidine nucleotides in the tRNA structure and A represents the adenine base.

Discussion

The centre of domain V is exceptionally rich in conserved nucleotides (Figures 1 and 7), several of which have been implicated, directly or indirectly, in the binding sites of antibiotics that affect peptidyl transfer. Each mutation had a profound effect on the growth rate of the host cells. Expression of the RNAs bearing the mutations A_{2060} → C and A_{2450} → C rendered cells inviable while the changes G_{2502} → A and A_{2503} → C produced much slower cell growth rates. For the two lethal mutations, there was a strong selection against the survival of plasmids pLK35V5 and pLK35V2 in HB101 cells (Table I); few colonies formed and they were variable in size. These viable cells probably exhibit plasmid deletions which also occurred frequently during initial attempts to transform the two mutated plasmids into HB101.

In an attempt to interpret these dramatic effects on cell growth rate we consider the mutants at two levels. First, the structure–function relationships between the mutagenized RNA region, the chloramphenicol binding site and the peptidyl transfer centre are established. Second, an attempt is made to explain how single mutations in the peptidyl transfer region render cells sick or inviable despite the presence of seven chromosome-coded rRNA operons.

Is the RNA site involved in chloramphenicol binding?

Originally, the nucleotides were selected for mutation because they occurred at, or adjacent to, nucleotides that have been implicated directly, or indirectly, in chloramphenicol binding. The A_{2060} → C and A_{2450} → C

mutants could not be tested for resistance to chloramphenicol because expression of the mutated 23S RNA was lethal to the cells. The $G_{2502} \rightarrow A$ mutant was tested and there was no effect on the chloramphenicol phenotype. However, the adjacent $A_{2503} \rightarrow C$ transversion did produce a chloramphenicol-resistant phenotype in the HB101 cells. Since the same natural mutation in yeast mitochondrial rRNA (Figure 1) generated the same effect, this nucleotide is conserved functionally as well as structurally in *E.coli*.

In total, seven single mutations within the central loop of domain V of *E.coli* 23S RNA have been correlated with chloramphenicol resistance (Figure 1). Direct mapping of the chloramphenicol binding site, using chemical reagents, also revealed protection effects at the four positions A_{2059}, A_{2062}, A_{2451} and G_{2505} and an enhanced reactivity at A_{2058} within the same region (Moazed and Noller, 1987a). The small chloramphenicol molecule (Figure 8) cannot interact simultaneously with all of these nucleotides and it is likely, therefore, that they all contribute to RNA tertiary structure at the chloramphenicol binding site. The presence of such an active RNA site is supported by the structural data (Table IV, Figure 7). These show that parts of the RNA region are fairly reactive in ribosomes, compared with other RNA domains (e.g. Egebjerg *et al.*, 1987) and, therefore, probably not masked by proteins.

Does chloramphenicol block peptidyl transfer?

The evidence implicating chloramphenicol in binding at the peptidyl transfer site derives mainly from its adverse effect on puromycin action in the 'fragment' reaction, where peptide bonds are formed between the aminoacyl tRNA fragment and puromyin on the 50S subunit in the presence of methanol (reviewed by Vazquez, 1979).

In an attempt to explain this effect we deduced a model for chloramphenicol binding at the peptidyl transfer centre. As has been noted before (Spirin, 1986), part of the chloramphenicol molecule can mimic a peptide bond. Here we suggest that the antibiotic binds at the ribosomal site where the peptide bond forms, and thereby prevents correct positioning of the aminoacyl groups of the tRNAs bound in the A- and P-sites, without weakening tRNA binding. The site of peptide bond formation is probably a precisely defined structural locus while the surrounding structure must be more flexible to accommodate the various amino acid side chains. The D-*threo* configuration of chloramphenicol, which is the only active stereoisomer (Vazquez, 1979), is co-structural with the L-form of amino acids. The encircled groups in the chloramphenicol molecule (Figure 8) can be substituted without loss of activity and are, therefore, not essential for ribosome binding. The amide and phenyl groups, however, are essential and, in the proposed model, the amide group binds at the site of the newly formed peptide bond and the phenyl group is located nearby on the ribosome. Competition between chloramphenicol and puromycin could involve the phenyl group since it is located in a similar position in puromycin when it mimics the 3′ end of aminoacyl-tRNA at the A-site. Furthermore, anisomycin, which inhibits peptide bond formation in eukaryotes, also exhibits an identical phenyl entity (Figure 8). Moreover, its ribosomal binding site probably overlaps with that of chloramphenicol since two point mutations in the rRNA, which induce anisomycin resistance, coincide with those conferring chloramphenicol resistance (Figure 1). A ribosomal binding site for a phenyl group at this position could also explain why chloramphenicol inhibits poly(U)- less than poly(A)- or poly(C)-directed synthesis (Speyer *et al.*, 1963; Kucan and Lipmann 1964; Vazquez, 1966) since poly(U)-encoded phenylalanine has a similarly located phenyl group and, in contrast to the poly(A)- and poly(C)-encoded lysine and proline, it can compete with, and displace, chloramphenicol during peptide bond formation. This view receives support from the results of Kucan and Lipmann (1964) who showed that poly(UA)-coded synthesis was less inhibited than poly(UC)-coded synthesis. Both code for phenylalanine but, in addition, the former codes for tyrosine which also has a phenyl group at a similar position.

How do the mutations inhibit host cell growth?

We assume that all of the growth inhibition effects derive from the assembly of ribosomes that are functionally defective in the peptidyl transfer region. Thus cells will waste energy in the production of partially active or inactive ribosomes. The nature of the defects in the 50S subunits apparently differs for the four mutants. Although each mutant RNA assembled into 50S subunits, the stabilities of the 70S ribosomes varied (Table III). For the two lethal mutants, low levels of the $A_{2060} \rightarrow C$ RNA and no $A_{2450} \rightarrow C$ RNA were detected in 70S ribosomes, which suggests that defects occurred at the subunit interaction site of the 50S subunits. This interpretation concurs with peptidyl transfer occurring at the subunit interface and is reinforced by the evidence for both wild-type and the $A_{2503} \rightarrow C$ mutant producing less stable 70S ribosomes when grown in chloramphenicol (Figure 5B,D); presumably the antibiotic influences the assembly and resultant structure of the centre of domain V RNA. Finally, the partial selection against incorporation of the $G_{2502} \rightarrow A$ mutant RNA into polysomes could also reflect an altered subunit−subunit interaction.

The structural study of the domain V region of the mutant RNA-enriched ribosomes isolated from the $G_{2502} \rightarrow A$ and $A_{2503} \rightarrow C$ mutants provided evidence for the occurrence of minor conformational changes (Table IV). Three nucleotides in each mutant RNA exhibited altered reactivities. These included the mutated nucleotide and an enhanced reactivity of A_{2453} to DEP that was common to both mutants. These altered sites all occur in the central circle (Figure 7) and they neighbour sites previously implicated in chloramphenicol binding. Since a comparison with data obtained from wild-type ribosomes (Table IV) suggests that the full complement of ribosomal proteins was assembled, we infer that the deleterious effects of the mutations resulted from disruption, or weakening, of RNA interactions within the centre of domain V or between this region and other components of the translational apparatus.

Regulatory considerations

The two lethal mutations are paradoxical. Why are they lethal despite the presence of seven chromosome-coded RNA operons? It is very difficult to explain the lethal effects at the level of transcriptional regulation of rRNA (Cole *et al.*, 1987 and references therein). The most likely explanation is that a defect occurs at the translational level which affects, directly or indirectly, the active unmutated ribosomes. Thus, defective 50S subunits or unstable 70S ribosomes could sequester a factor, reduce the fidelity of translation or, possibly, form a block on the mRNA.

The $A_{2503} \rightarrow C$ mutant also provides a paradox. The mutant ribosomes were active *in vivo* in the presence of chloramphenicol, and also showed impaired activity in its absence. Curiously, the ribosomes accumulated high levels of mutant RNA in the absence of chloramphenicol (>90%). Neither recombination in the HB101 cells (*recA*$^-$), nor an enhanced plasmid copy number resulting from a longer doubling time (Lin-Chao and Bremer, 1986), are likely to explain this effect. Importantly, the observation does not accord with the relative gene dosages of plasmid and chromosome-coded RNAs (Gourse *et al.*, 1985), nor with their co-regulation (Jinks-Robertson *et al.*, 1983).

Materials and methods

Bacterial strains, plasmids and M13 vectors

E.coli strains HB101 (Maniatis *et al.*, 1982), C_{600} (λcI857, S7) (kindly provided by K.G.Gausing) and M5219 (λ bio 252 cI857 → HI) (Remaut *et al.*, 1981) were used as plasmid hosts. Growth medium contained 10 g tryptone (Difco), 5 g yeast extract (Difco) and 5 g NaCl per litre. Antibiotics were from Sigma. Plasmids and the replicative form of M13 recombinants were isolated by standard procedures (Maniatis *et al.*, 1982). Single-stranded M13 phage DNA was purified essentially as described by Sanger *et al.* (1980). Restriction enzymes were from Amersham.

Plasmid cloning, expression and sequencing

pDV was derived from pKK3535 (Brosius *et al.*, 1981) by deleting a *BclI–EcoRI* fragment and a *NaeI* fragment. This removed a *PstI* site leaving a unique *PstI* site in the Amp^r gene that was useful for later cloning. pDV was digested by *PvuII* and the smaller of two fragments was isolated on an agarose gel, extracted and ligated to yield plasmid pSV (Figure 2A). A gapped-duplex form of the plasmid was constructed for mutagenesis by first digesting pSV with *PstI* in the *Amp* gene and dephosphorylating. Another aliquot was then digested with *AvaI* and a 750-bp fragment was excised. The fragments were mixed, denatured by heating and renatured to yield heteroduplexes. The gapped-duplex form was separated on an agarose gel and extracted. After mutagenizing plasmid pSV (see below), it was digested with *PstI* and *PvuII* and the mutated 2.5-kb fragment was isolated and back-cloned into the original pDV plasmid (Figure 2A). Mutated fragments that resisted this back-cloning were excised with *XbaI* and *SmaI* and religated to a fragment which was obtained by digesting of plasmid pLK35 with *BamHI* followed by treatment with the Klenow enzyme and dNTP's and finally digested with *XbaI*; pLK35 was derived from pNO2680 (Gourse *et al.*, 1985) by deleting a 0.9-kb *NaeI–BamHI* fragment in the pBR322 moiety of the plasmid which exhibits a λ phage P_L promoter before the *rrnB* genes. Procedures for restriction enzyme digestion, gel electrophoresis and ligation were described by Maniatis *et al.* (1982). Competent cells were prepared according to a standard procedure (Hanahan, 1985). All point mutations induced in plasmids were confirmed by DNA sequencing, either after cloning of the mutated fragment in a M13 phage or by sequencing directly on the mutated plasmid (Sanger *et al.*, 1977).

Primer-directed mutagenesis

Four primers (5′-GGGGTCG$_{2060}$TTCCGTC-3′, 5′-CAGCCTGT(A + G)$_{2450}$ATCCCC-3′, 5′-GCCGACA(G + C)$_{2502}$CGAGGTGCC-3′ and 5′-GACCCGACAT(G + T)$_{2503}$GAGGTGCC-3′) were synthesized by the solid-phase phosphotriester method (Sproat and Gait, 1984) on a support of controlled pore glass. The primers were used to mutagenize positions 2060, 2450, 2502 and 2503 in *E.coli* 23S RNA on a gapped-duplex plasmid (Inouye and Inouye, 1987). After transforming, colonies were screened for mutations by dot-blot hybridization in which colonies were transformed to a Gene-Screen membrane (NEN). The filter was denatured in 0.2 M NaOH, 0.6 M NaCl, neutralized in 0.5 M Tris–HCl, pH 7.5, 1.5 M NaCl, and rinsed before baking the membrane for 3 h at 80°C. Prehybridization and hybridization procedures (Zoller and Smith, 1982) were used. We screened for mutants by washing filters at increasing temperatures; plasmids with potential mutations were then retransformed.

Each mutation was confirmed by DNA sequencing (Sanger *et al.*, 1977) after cloning the 2.5-kb *PvuII–PstI* fragments from the mutant plasmids into an M13mp9 vector. rRNA was sequenced by primer-directed reverse transcriptase (Zimmern and Kaesberg, 1978).

Preparation of active ribosomes and polysomes

Cultures of HB101/pDV (with and without 4 μg/ml chloramphenicol), HB101/pDV4 and HB101/pDV3 (with and without 7.5 μg/ml chloramphenicol) were grown to ~0.7 A_{650} units. Ribosomes were extracted, salt-washed and separated by gel filtration on Sephacryl S-200 (Pharmacia) and stored at −80°C in 'polymix' buffer (5 mM K_3PO_4, 5 mM $MgCl_2$, 0.5 mM $CaCl_2$, 8 mM putrescine, 1 mM spermidine, 5 mM NH_4Cl, 95 mM KCl, 1 mM dithioerythreitol, pH 7.5) (Jelenc, 1980). Ribosome/subunit profiles were investigated as follows: 33 μg ribosomes were diluted to 50 μl with 30 mM Tris–HCl, pH 7.5, 10 mM $MgCl_2$, 100 mM NH_4Cl and centrifuged in a Beckman SW60 Ti rotor for 15 h at 20 000 rev/min and 5°C in a 5–20% (w/v) sucrose density gradient containing the same buffer. Polysomes were extracted and separated on 15–30% (w/v) sucrose gradients containing 50 mM Tris–HCl (pH 7.5), 10 mM $MgCl_2$, 60 mM KCl for 4.5 h at 20 000 rev/min and 4°C in a SW 28 rotor (Godson and Sinsheimer, 1967). All sucrose gradients were eluted and analysed at 260 nm in a Gilson Spectrochrom M spectrophotometer.

Probing with ribonucleases and chemical reagents

Samples containing 15 μg ribosomes were partially digested with 0.015 U RNase T_2 (Sankyo) in 20 μl 30 mM Tris–HCl (pH 7.8), 10 mM $MgCl_2$, 300 mM KCl ($T_{30}M_{10}K_{300}$) for 30 min at 0°C or 0.015 U CV RNase in 20 μl $T_{30}M_{10}K_{300}$ (pH 7.8) for 60 min at 0°C. Digestions were stopped by extracting twice with phenol saturated in 250 mM sodium acetate, pH 6.0, and RNA was precipitated twice with 2.5 vol ethanol.

Samples containing 8 μg ribosomes were treated under the chemical conditions described by Egebjerg *et al.* (1987).

Diethylpyrocarbonate (DEP, Eastman Kodak). Twenty microlitres was added to the sample in 200 μl 70 mM Hepes (pH 7.2), 10 mM $MgCl_2$, 270 mM KCl ($H_{70}M_{10}K_{270}$). The mixture was incubated for 15 min at 20°C and the reaction was stopped by extracting once with ether and precipitating with 2.5 vol ethanol.

Dimethylsulfate (DMS, Merck). One microlitre was added to the sample in 300 μl 70 mM sodium cacodylate (pH 7.4), 10 mM $MgCl_2$, 270 mM KCl ($C_{70}M_{10}K_{270}$). The mixture was incubated for 5 min at 30°C and the reaction was stopped by adding 2-mercaptoethanol.

Carbodiimide (CMCT, Sigma). Twenty microlitres of 42 mg/ml 1-cyclohexyl-3-(2-morpholinoethyl)-carbodiimide-metho-*p*-toluene sulphonate was added to the sample in 20 μl $T_{30}M_{10}K_{300}$ (pH 7.8). The mixture was maintained at 30°C for 1.5 h and the reaction was stopped by precipitating with 2.5 vol ethanol.

Kethoxal (Serva). Three microlitres of Kethoxal (35 mg/ml) was added to the sample in 200 μl $H_{70}M_{10}K_{270}$ (pH 7.8). The mixture was incubated for 5 min at 30°C and the reaction was stopped by precipitation with 2.5 vol ethanol. All modified samples were extracted twice with phenol, once with chloroform and then the RNA was precipitated with 2.5 vol ethanol before storing in 10 mM Tris–HCl (pH 7.5), 0.1 mM EDTA at −80°C.

Reverse transcription and sequence analysis

Ten microlitres of annealing mixture containing 1 μg RNA in 40 mM Tris–HCl (pH 7.5), 40 mM KCl and 0.75 pmol labelled primer was heated for 30 s at 95°C and then maintained for 20 min at 50°C. Three microlitres of annealing mixture was added to 2 μl extension mixture [0.5 mM dTTP, dATP, dGTP and dCTP; 125 mM Tris–HCl, pH 7.5, 25 mM $MgCl_2$, 5 mM DTT and 1.0 U AMV reverse transcriptase (Life Sciences, FL)]. The sample was incubated for 25 min at 37°C. Sequencing samples were prepared by adding 1 μl of 0.67 mM ddATP, 0.67 mM ddTTP, 0.44 mM ddGTP or 0.22 mM ddCTP respectively to the above reaction mixtures. The reaction was stopped by adding 5 μl gel loading buffer (10 mM EDTA, 0.05% bromophenol blue, 0.05% xylene cyanol in deionized formamide). Samples were run on 6.6% thermostatted polyacrylamide gels.

Acknowledgements

Annette Andersen is thanked for her excellent technical help. Steve Douthwaite kindly provided the plasmid pLK35. Niels Larsen, Jan Egebjerg and Henrik Leffers contributed their helpful counsel. In particular, we thank Jan Egebjerg for sharing and discussing his own detailed structural studies on domain V. Solveig Kjær's and Kirsten Skov's help with the manuscript was appreciated. B.V. received a licentiate grant from the Carlsberg

Foundation and was subsequently supported by the Danish Centre for Microbiology. The research was supported by grants from both the Danish Medical Research Council and the Carlsberg Foundation.

References

Barta,A., Steiner,G., Brosius,J., Noller,H.F. and Keuchler,E. (1984) *Proc. Natl. Acad. Sci. USA*, **81**, 3607–3611.
Blanc,H., Adams,C.A. and Wallace,D.C. (1981) *Nucleic Acids Res.*,**9**, 5785–5795.
Brosius,J., Ullrich,A., Raker,M.A., Gray,A., Dull,T.J., Gutell,R.R. and Noller,H.F. (1981) *Plasmid*, **6**, 112–118.
Cole,J.R., Olsson,C.L., Hershey,J.W.B., Grunberg-Manago,M. and Nomura,M. (1987) *J. Mol. Biol.*, **198**, 383–392.
Dujon,B. (1980) *Cell*, **20**, 185–197.
Egebjerg,J., Leffers,H., Christensen,A., Andersen,H. and Garrett,R.A. (1987) *J. Mol. Biol.*, **196**, 125–136.
Endo,Y. and Wool,I.G. (1982) *J. Biol. Chem.*, **257**, 9054–9060.
Endo,Y., Mitsui,K., Motizuki,M. and Tsurugi,K. (1987) *J. Biol. Chem.*, **262**, 5908–5912.
Ettayebi,M., Prasad,S.M. and Morgan,A. (1985) *J. Bacteriol.*, **162**, 551–557.
Godson,G.N. and Sinsheimer,R.L. (1967) *Biochim. Biophys. Acta*, **149**, 489–495.
Gourse,R.L., Takebe,Y., Sharrock,R.A. and Nomura,M. (1985) *Proc. Natl. Acad. Sci. USA*, **82**, 1069–1073.
Hanahan,D. (1985) In Glover,D.M. (ed.), *DNA Cloning: A Practical Approach*. IRL Press, Oxford, Vol. 1, pp. 109–135.
Hummel,H. and Böck,A. (1987) *Nucleic Acids Res.*, **15**, 2431–2443.
Inouye,S. and Inouye,M. (1987) In Narang,S.A. (ed.), *Synthesis and Applications of DNA and RNA*. Academic Press, New York.
Jacob,W.F., Santer,M. and Dahlberg,A.E. (1987) *Proc. Natl. Acad. Sci. USA*, **84**, 4757–4761.
Jelenc,P.C. (1980) *Anal. Biochem.*, **105**, 369–374.
Jinks-Robertson,S., Gourse,R.L. and Nomura,M. (1983) *Cell*, **33**, 865–876.
Kearsey,S.E. and Craig,I.W. (1981) *Nature*, **290**, 607–608.
Koike,K., Taira,M., Kuchino,Y., Yaginuma,K., Sekiguchi,T. and Kobayashi,M. (1983) In Schweyen,R.J., Wolf,K. and Kaudewitz,F. (eds), *Mitochondria*. Walter de Gruyter, Berlin, pp. 372–387.
Kucan,Z. and Lipmann,F. (1964) *J. Biol. Chem.*, **239**, 516–520.
Leffers,H., Kjems,J., Østergaard,L., Larsen,N. and Garrett,R.A. (1987) *J. Mol. Biol.*, **194**, 43–61.
Lin-Chao,S. and Bremer,H. (1986) *Mol. Gen. Genet.*, **203**, 143–149.
Maniatis,T., Fritsch,E.F. and Sambrook,J. (1982) *Molecular Cloning: A Laboratory Manual*. Cold Spring Harbor Laboratory Press, Cold Spring Harbor.
Moazed,D. and Noller,H.F. (1986) *Cell*, **47**, 985–994.
Moazed,D. and Noller,H.F. (1987a) *Biochimie*, **69**, 879–884.
Moazed,D. and Noller,H.F. (1987b) *Nature*, **327**, 389–394.
Moazed,D., Stern,S. and Noller,H.F. (1986) *J. Mol. Biol.*, **187**, 399–416.
Noller,H.F. (1984) *Annu. Rev. Biochem.*, **53**, 119–162.
Noller,H.F. and Chaires,J.B. (1972) *Proc. Natl. Acad. Sci. USA*, **69**, 3115–3118.
Pestka,S. (1974) *Ant. Agents Chemother.*, **5**, 255–267.
Remaut,E., Stanssens,P. and Fiers,W. (1981) *Gene*, **15**, 81–93.
Sanger,F., Nicklen,S. and Coulsen,A.R. (1977) *Proc. Natl. Acad. Sci. USA*, **74**, 5463–5467.
Sanger,F., Coulson,A.R., Barrell,B.G., Smith,A.J.H. and Roe,B.A. (1980) *J. Mol. Biol.*, **143**, 161–178.
Schleif,R.F. (1968) *J. Mol. Biol.*, **37**, 119–129.
Senior,B.W. and Holland,I.B. (1971) *Proc. Natl. Acad. Sci. USA*, **68**, 959–963.
Shine,J. and Dalgarno,L. (1974) *Proc. Natl. Acad. Sci. USA*, **71**, 1342–1346.
Sigmund,C.D., Ettayebi,M. and Morgan,A. (1984) *Nucleic Acids Res.*, **12**, 4653–4663.
Skinner,R.H. and Cundliffe,E. (1982) *J. Gen. Microbiol.*, **128**, 2411–2416.
Slott,E.F., Shade,R.O.,Jr and Lansman,R.A. (1983) *Mol. Cell. Biol.*, **3**, 1694–1702.
Sor,F. and Fukuhara,H. (1982) *Nucleic Acids Res.*, **10**, 6571–6577.
Sor,F. and Fukuhara,H. (1984) *Nucleic Acids Res.*, **12**, 8313–8318.
Speyer,F.J., Lengyel,P., Basilo,C., Wahba,A.J., Gardner,R.S. and Ochoa,S. (1963) *Cold Spring Harbor Symp. Quant. Biol.*, **28**, 559–567.
Spirin,A.S. (1986) *Ribosome Structure and Protein Biosynthesis*. W.A. Benjamin, Menlo Park, Calif. pp. 263–265.
Sproat,B.S. and Gait,M.J. (1984) In Gait,M.J. (ed.), *Oligonucleotide Synthesis: A Practical Approach*. IRL Press, Oxford, pp. 83–115.
Vazquez,D. (1966) *Biochim. Biophys. Acta*, **114**, 289–295.
Vazquez,D. (1979) *Inhibitors of Protein Synthesis*, Springer-Verlag, Berlin.
Vester,B. and Garrett,R.A. (1987) *Biochimie*, **69**, 891–900.
Zimmern,D. and Kaesberg,P. (1978) *Proc. Natl. Acad. Sci. USA*, **75**, 4257–4261.
Zoller,M.J. and Smith,M. (1982) *Nucleic Acids Res.*, **10**, 6487–6500.

Received on June 9, 1988; revised on August 15, 1988